

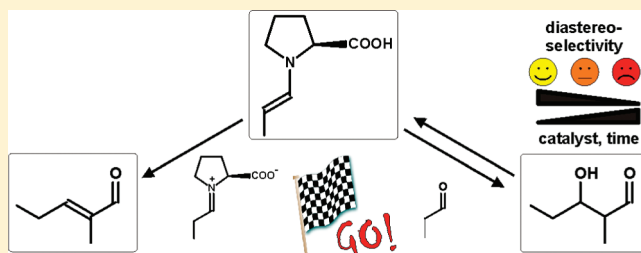
NMR Investigations on the Proline-Catalyzed Aldehyde Self-Condensation: Mannich Mechanism, Dienamine Detection, and Erosion of the Aldol Addition Selectivity

Markus B. Schmid, Kirsten Zeitler,* and Ruth M. Gschwind*

Institut für Organische Chemie, Universität Regensburg, Universitätsstr. 31, D-93053 Regensburg, Germany

S Supporting Information

ABSTRACT: The proline-catalyzed self-condensation of aliphatic aldehydes in DMSO with varying amounts of catalyst was studied by in situ NMR spectroscopy. The reaction profiles and intermediates observed as well as deuteration studies reveal that the proline-catalyzed aldol addition and condensation are competing, but not consecutive, reaction pathways. In addition, the rate-determining step of the condensation is suggested to be the C–C bond formation. Our findings indicate the involvement of two catalyst molecules in the C–C bond formation of the aldol condensation, presumably by the activation of both the aldol acceptor and donor in a Mannich-type pathway. This mechanism is shown to be operative also in the oligomerization of acetaldehyde with high proline amounts, for which the first in situ detection of a proline-derived dienamine was accomplished. In addition, the diastereoselectivity of the aldol addition is evidenced to be time-dependent since it is undermined by the retro-aldolization and the *competing* irreversible aldol condensation; here NMR reaction profiles can be used as a tool for reaction optimization.



INTRODUCTION

Detailed insights into the mechanisms of both intended organic reactions and unwanted side reactions are of utmost importance for better control and for the rational optimization of reaction conditions in synthetic organic chemistry. Nevertheless, such knowledge is often difficult to obtain since it is in many cases intimately connected to the detection of elusive reaction intermediates. Accordingly, in the growing field of asymmetric organocatalysis,^{1–5} where the development of novel synthetic applications has been predominant over mechanistic investigations, reaction optimization often appears to be rather empirical than rational. For instance, the proline-catalyzed intermolecular aldol reaction,⁶ archetypical for the concept of enamine catalysis by secondary amines in general,^{7–12} has been reported right from its beginnings to be accompanied by the aldol condensation reaction;⁶ yet, despite proline being an important bifunctional catalytic system of acknowledged model character, whose mechanistic features have been and are still a matter of intensive theoretical^{13–16} and experimental^{17–23} studies, it has not been clarified unambiguously up to now whether the aldol addition and the aldol condensation must be regarded as *competing* or as *consecutive* reactions.²⁴ However, such knowledge should help to rationally optimize reaction protocols for the suppression of the aldol condensation as an unwanted side reaction in asymmetric aldol addition reactions.²⁵ On the other hand, based on a better mechanistic understanding of the ongoing reactions, one may improve the outcome of organocatalytic carbonyl condensations.²⁶

The potential of this rediscovered route for the generation of versatile α,β -unsaturated carbonyl compounds has been recognized and successfully exploited recently.^{27,28} Concerning the mechanistic understanding of the amine-catalyzed aldol condensation, it has been shown that α,β -unsaturated ketones are not obtained from the corresponding aldol products by treatment with proline in acetone/chloroform.²⁹ In addition, from a kinetic study on the pyrrolidine-catalyzed aldehyde-aldehyde condensation in chloroform, evidence has been reported that the reaction is of second order in the catalyst concentration.²⁷ A second-order pathway for the C–C bond-forming step was also suggested by kinetic studies on the acetaldehyde condensation in aqueous and salt solution with high catalyst concentrations.³⁰ On the basis of these experimental findings, Mannich-like mechanisms for the proline-catalyzed aldol condensation have been proposed in contrast to the presumably more intuitive pathway of aldol addition and subsequent dehydration. Nonetheless, comprehensive mechanistic studies were not possible so far, in particular since more detailed investigations have been impeded for a long time by the inability to detect and characterize proline enamines in situ. Only recently could this key intermediate of most of the mechanistic proposals be snared in situ by means of NMR spectroscopy.²⁰ It should now allow access to more detailed insights into the underlying reaction mechanism.

Received: February 25, 2011

Published: March 29, 2011

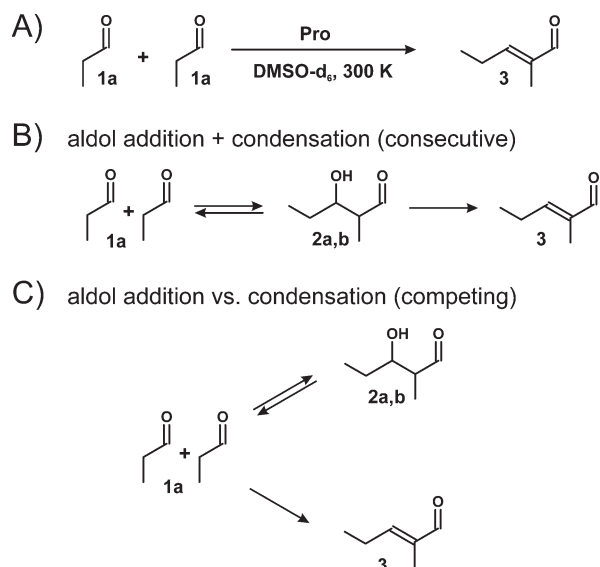
Here, we present our mechanistic studies on the proline-catalyzed self-condensation of aliphatic aldehydes in DMSO. Starting from the monomeric aldehyde or from the aldol dimer, online-NMR spectroscopy was applied to monitor the aldol addition, the aldol condensation, and the retro-aldolization, which were shown to proceed in parallel within our samples. This was achieved with the help of characteristic well-resolved proton resonances of the different species (see Figure S2 in the Supporting Information). Based on the reaction profiles obtained and the intermediates observed, we can now thoroughly interpret the ongoing events in the reaction mixtures with regard to the formation pathway of the condensation product. Furthermore, a deuteration study by adding small amounts of D₂O to the reaction mixtures allowed us to follow the progress of the α -deuteration via the reaction intermediates and to track the accumulation of deuterium in the reaction products. The observed reaction profiles and the degrees of deuteration rule out the existence of an aldol addition–dehydration pathway for the formation of the condensation product under proline catalysis in DMSO. Instead, a Mannich-like mechanism, most probably via a double aldehyde-activation, is evidenced for the proline-catalyzed self-condensation of aliphatic aldehydes in DMSO. In addition, the first detection of a proline-derived dianamine is presented. In the context of parallel activation and reaction pathways, using NMR reaction profiles we demonstrate that the selectivity of the aldol addition reaction is dependent on the reaction time because of the competition between the reversible aldol addition and the irreversible aldol condensation pathway.

■ RESULTS AND DISCUSSION

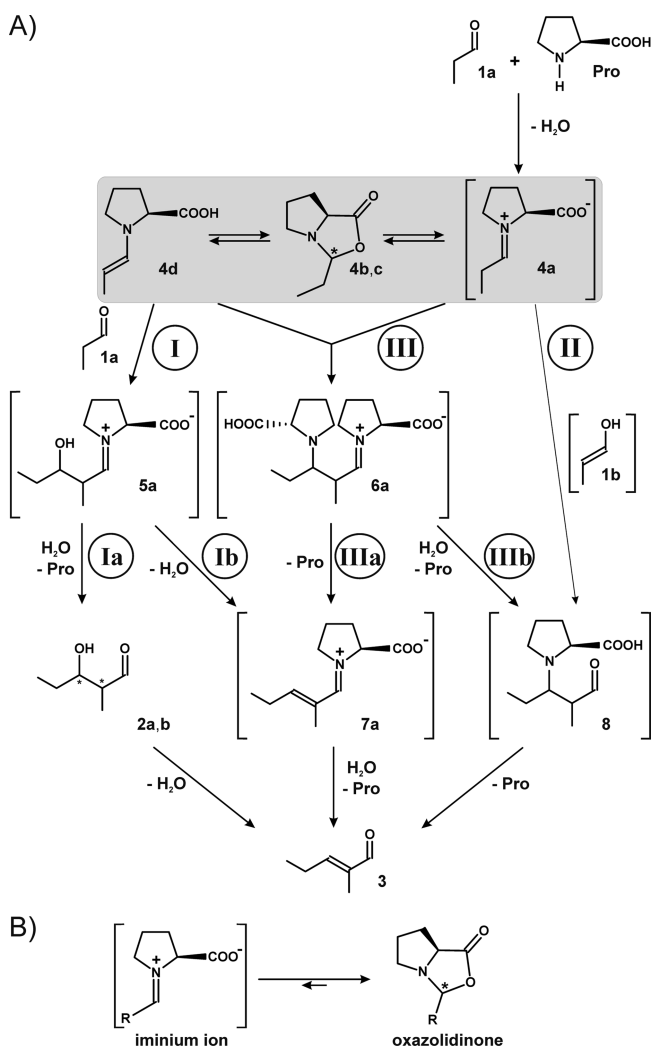
Model Reaction and General Mechanistic Considerations.

As a model system for our investigations on the proline-catalyzed self-condensation of aliphatic aldehydes, propionaldehyde **1a** was selected as the starting material ($c = 50$ mM), 100 mol % of L-proline as the amine catalyst and DMSO- d_6 at 300 K as the

Scheme 1. (A) Model Reaction Investigated: Proline-Catalyzed Self-Condensation of Propionaldehyde 1a. (B) and (C) Aldol Condensation as a Process That Is Either Consecutive or Competing with the Aldol Addition, Respectively



Scheme 2. (A) Possible Mechanistic Pathways for the Process of Scheme 1A, Proposed in the Literature^{27,29,31–37} (Note: Species That Could Not Be Detected in This Study Are Shown in Brackets). (B) Commonly Proposed Iminium—Oxazolidinone Equilibrium



solvent (Scheme 1A). This choice was based on our recent study that had allowed us to detect in situ the elusive proline–enamine and further intermediate species in the intermolecular aldol reaction for the first time.²⁰ By thus presenting new options for the interpretation of reaction profiles, these experimental conditions were expected to also bring forward the mechanistic understanding of the proline-catalyzed aldehyde–condensation reaction.

As a first simplistic issue, the relationship between the proline-catalyzed aldol addition and the aldol condensation should be addressed, i.e., whether the aldol addition and aldol condensation are consecutive (Scheme 1B) or competing (Scheme 1C) reaction steps. More detailed considerations on the potential pathways of the proline-catalyzed aldehyde self-condensation have led to the three basic mechanistic pathways proposed in the literature (Scheme 2A).^{27,29,31–37} They can be classified by the nature of the species that are involved in the C–C bond-forming steps into an aldol pathway (I), a Mannich pathway (II), and a double-activation Mannich-type pathway (III).

Pathway I initially constitutes the commonly accepted mechanism of the proline-catalyzed intermolecular aldol reaction; it is characterized by the addition of the catalyst-derived enamine **4d** of the donor aldehyde to the acceptor aldehyde molecule **1a** and is completed by hydrolysis and dehydration (or vice versa), like the classical aldol condensation reaction.^{33–35}

Pathway II corresponds to a textbook Mannich mechanism, in which the enol tautomer **1b** of the donor aldehyde adds to the iminium ion **4a**, formed from the acceptor aldehyde and the amine catalyst, followed by elimination of the catalyst.^{29,31,32} A third mechanistic alternative, described by pathway III,^{27,36,37} has been pointed out recently: It resembles the Mannich pathway II but comprises the simultaneous activation of both the donor and the acceptor aldehyde as an enamine **4d** and an iminium ion **4a**, respectively, and subsequent elimination and hydrolysis steps.³⁸

Forward Aldol Addition and Condensation. To distinguish between the three proposed mechanisms, we have employed our recently gained knowledge on the observation of intermediates in proline-catalyzed aldol reactions.²⁰ On this basis, a very simple kinetic consideration should help us to obtain first insights into potential condensation reaction pathways: Whatever the exact underlying mechanism of the formation of the enal **3** may be, a certain correlation between the concentration of the intermediates involved in the rate-determining step and the formation rate of **3**, i.e., the slope of its NMR-derived concentration–time curve, should be expected. To apply this criterion to the different potential reaction pathways, we conducted the self-aldolization/condensation of propionaldehyde with different amounts of L-proline (100, 50, 20, and 10 mol %) in DMSO-*d*₆ at 300 K inside an NMR tube and monitored the progress of the reactions by one-dimensional proton spectra. For all the different proline concentrations applied as well as for butyraldehyde as the starting material with 100 mol % of proline, very similar characteristic features of the reaction progress were monitored. (Exemplary results for 100 mol % of proline are shown in Figure 1; see Figures S1 and S3 in the Supporting Information for the results of the other experimental setups.) First, the consumption of the starting material **1a** and the steady decrease of the concentration of the proline-derived propionaldehyde intermediates (the enamine **4d** and the isomeric oxazolidinones **4b,c**; Figure 1A) are observed. In addition, the formation of two product oxazolidinones **5b,c** (among others) and of the diastereomeric aldol dimers **2a,b** is evidenced as well as their disappearance (Figure 1B; maximum concentrations of **5b,c** after about 100 and 200 min and of **2a,b** after about 70 and 100 min, respectively).

Finally, the aldehyde self-condensation product **3** is formed irreversibly (Figure 1C) in about 90% yield after 12 h (The molar ratio on the y axis refers to the initial concentration of the aldehyde **1a**; see the Supporting Information for observations about aldehyde substitution effects on the reactivity and the enal *E/Z* selectivity).

In a previous study on a crossed-aldolization/-condensation of aldehydes,²⁷ the constant ratio of the aldol and the condensation product throughout the reaction time could be interpreted as an indication of the competition between the two reaction pathways. However, in the case of our self-aldolization/-condensation this argument cannot be applied since **3** is the only product of the reaction, while **2a,b** vanish again, either because of dehydration or because of retro-aldolization (Scheme 1B,C). Thus, the issue of whether the aldol addition and the aldol condensation are consecutive or competing reaction steps must be addressed by

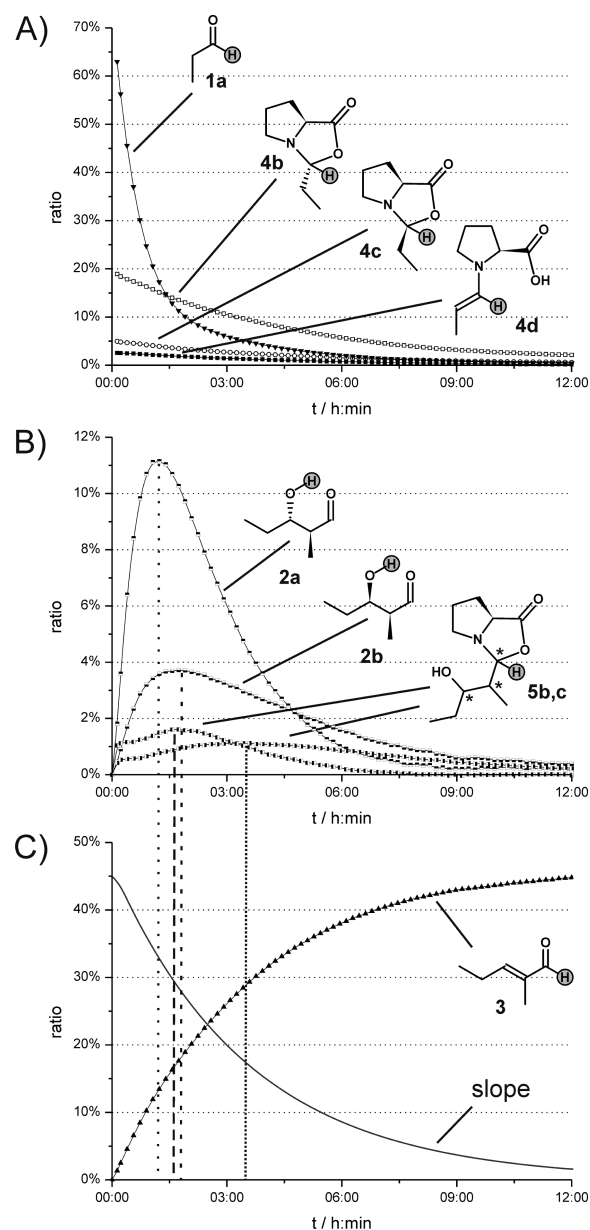


Figure 1. Reaction profile of the proline-catalyzed self-aldolization/condensation of propionaldehyde **1a** with 100 mol % L-proline in DMSO-*d*₆ at 300 K: (A) starting material and intermediates derived thereof, (B) aldol dimers and related oxazolidinones, and (C) condensation product and the slope (displayed in arbitrary units) of its buildup curve, which corresponds to the formation rate of **3**. (Those protons whose resonances were used for the monitoring are highlighted in gray; see Figure S2 in the Supporting Information. Note: The total amount of C₃ moieties stemming from propionaldehyde, detected in the first spectrum, was set to 100%. Times of concentration maxima of **2a,b** and **5b,c** are marked with vertical dotted lines.)

other means. In view of the reaction profile of Figure 1, it is highly striking that the maximum concentration of the aldol dimers **2a,b** (after 75 and 105 min, respectively, Figure 1B) does not at all coincide with the maximum slope of the concentration–time curve of the condensation product **3**, i.e. with its rate of formation (right at the beginning of the reaction, Figure 1C). According to the criterion outlined above, reaction pathway Ia (the aldol addition–hydrolysis–dehydration sequence in Scheme 2A) can

hence clearly be ruled out as the major pathway for the formation of enal **3**. Accordingly, the decrease of the concentration of the aldol dimers **2a,b** must be due to retro-aldolization rather than dehydration. In analogy, reaction pathway 1b (the aldol addition—dehydration—hydrolysis sequence, Scheme 2A) can be analyzed with regard to its plausibility. For the formation of enal **3** from the product iminium **5a** via its dehydrated analogue **7a** in this pathway, the elimination of water should be rate determining since we could show previously by cross-peak evaluation in EXSY spectra²⁰ that the hydrolysis of iminium ions/oxazolidinones to the corresponding aldehydes is a fast process and that, in contrast, the dehydration of aldol dimers is significantly slower (see also the next paragraph). Accordingly, in case pathway 1b was operative, the maximum formation rate of **3** would be expected to correlate with the maximum concentration of the hypothetical iminium ion **5a** (undetected in this study) and thus with the concentration of the well-observed isomeric oxazolidinones **5b,c**, as suggested by the commonly proposed iminium—oxazolidinone equilibrium (Scheme 2B).²⁰ Under these premises, the observed discrepancy between the maximum of the concentration—time-curves of **5b,c** and the maximum rate of formation of **3** (cf. Figure 1B and 1C) again indicates that pathway 1b is not the main route of the proline-catalyzed aldehyde self-condensation, either. Instead, as the formation of **3** is the faster the higher the concentration of the reactant intermediates **4b,c,d** (cf. Figure 1A and 1C), processes involving these intermediates in the rate determining step are suggested by the monitored concentration—time curves. Altogether, as a first result and in agreement with a previous study on the pyrrolidine-catalyzed aldehyde self-condensation,²⁷ the kinetic profile of an equimolar reaction mixture of proline and propionaldehyde **1a** in DMSO evidences that the proline-catalyzed intermolecular aldol addition and aldol condensation are not consecutive, but rather competing reaction pathways (Scheme 1C).

Formal Dehydration of Aldol dimers via Retro-Aldolization. To corroborate this finding, we investigated in more detail whether the condensation product **3** could be generated from the aldol products **2a,b** under our experimental conditions. For that purpose, the aldol addition dimers **2a,b** were synthesized,³⁹ isolated as a mixture of diastereomers, dissolved in DMSO-*d*₆ inside an NMR tube, and exposed to benzoic acid or proline as potentially dehydrating additives. The events in the reaction mixtures were then again monitored by one-dimensional proton NMR spectra. First, we studied the influence of Brønsted acid addition: However, 100 mol % of benzoic acid, a previously employed cocatalyst in organocatalytic aldehyde self-condensations,^{27,32} virtually did not effectuate any dehydration of the aldol dimers **2a,b** over 15 h (data not shown). We conclude from this that the proline-catalyzed aldehyde condensation is not a Brønsted acid-catalyzed dehydration of aldol addition products. As a next approach, we added 100 mol % of L-proline to **2a,b** in DMSO-*d*₆. The concentration curves of the observed species in the reaction mixture are summarized in Figure 2.

In contrast to an early report on a similar approach in acetone/chloroform starting from a β -hydroxy ketone,²⁹ we could easily detect the formal dehydration of the β -hydroxy aldehydes **2a,b** in DMSO-*d*₆ under the influence of 100 mol % of proline: The concentrations of the aldol dimers **2a,b** decrease over time (Figure 2A), while the amount of the condensation product **3** increases in turn (Figure 2C).

However, the monomeric propionaldehyde **1a**, and—in agreement with our previous EXSY findings²⁰—the corresponding oxazolidinones **4b,c** and the enamine **4d** (Figure 2B) are observed

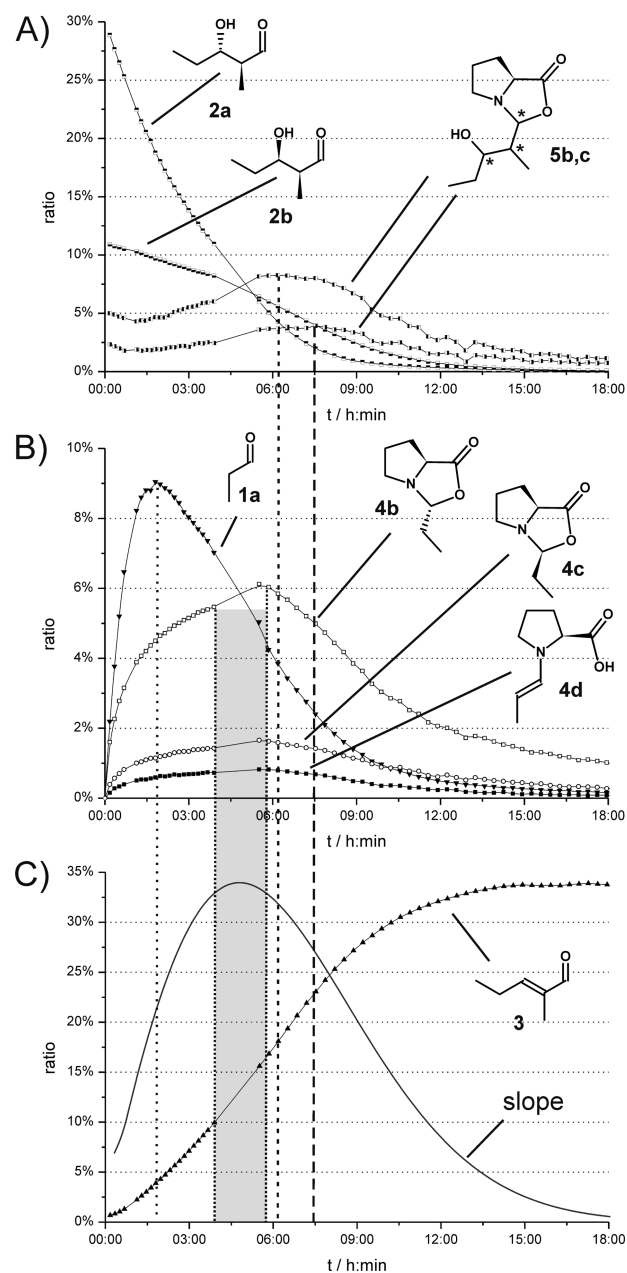


Figure 2. Reaction profile of the proline-catalyzed formal dehydration of the aldol addition dimers **2a,b** in DMSO-*d*₆ at 300 K under proline catalysis (100 mol %): (A) aldol dimers and related oxazolidinones, (B) propionaldehyde and intermediates derived thereof, and (C) condensation product and the slope (displayed in arbitrary units) of its buildup curve, which corresponds to the formation rate of **3**. (Notes: The total amount of C₃ moieties stemming from propionaldehyde, detected in the first spectrum, was set to 100%. Times of concentration maxima of **1a** and **4b,c,d** are marked with vertical dotted lines. The kinks in some of the curves are due to the temporary removal of the sample from the NMR spectrometer and the associated disturbances, resulting in a larger error range for the maximum concentration of **4b,c,d**.)

in the reaction mixture, too, being indicative of the readily occurring retro-aldol reaction under our experimental conditions. Thus, to clarify whether the condensation product **3** results from **2a,b** via a direct dehydration (Scheme 1B) or rather from a sequence of retro-aldol reaction and Mannich-type condensation

(Scheme 1C), the above-mentioned argumentation needs to be applied once more: In concordance with the findings for the forward aldol condensation (Figure 1), the maximum formation rate of **3** (Figure 2C), starting from the aldol dimers **2a,b**, does not coincide with the highest concentration of **2a,b** (at the very beginning of the reaction, Figure 2A) or the product oxazolidinones **5b,c**. This confirms that the major formation pathway of **3** is not the direct dehydration of **2a,b** (pathway 1a in Scheme 2A). Instead, the formation rate of **3** shows an induction period; its maximum is reached only after 4–5 h. Most interestingly, it is correlated to the maximum concentration of the intermediates **4b,c,d**. This supports the hypothesis that these species are involved in the rate-determining step of the proline-catalyzed aldehyde condensation.

Deuteration Experiments. Further evidence for the observed competition between the proline-catalyzed aldol addition and aldol condensation was collected from a deuteration study on the above-mentioned formal dehydration of the aldol dimers **2a,b**. In the case of a consecutive aldol condensation (Figure 3A, left), the degree of α' -deuteration of **3** is determined by the degree of α' -deuteration of **2a,b** (α' and β' refer to the α and β position of the former aldol acceptor moiety within the dimers **2a,b** and **3**, see Figure 3A), whereas in the case of a competing condensation pathway (Figure 3A, right), it is determined by the degree of α -deuteration of the aldol acceptor species (i.e., **1a** or **4a** in Scheme 2A). The latter case implies that there is not necessarily a causal relationship between the degrees of α' -deuteration of **2a,b** and **3** so that the degree of α' -deuteration of **3** may well exceed that of **2a,b**. In contrast, for our experimental approach starting from nondeuterated **2a,b**, the consecutive condensation pathway (Figure 3A, left) does not allow for a higher degree of α' -deuteration of **3** compared to **2a,b** because it can be assumed, following well-known kinetic isotope effects,⁴⁰ that the dehydration of α' -deuterated **2a,b** is not faster than the one of nondeuterated **2a,b**. Hence, the observation of a higher degree of α' -deuteration of **3** compared to **2a,b** would provide further strong evidence for the aldol condensation being in competition with the aldol addition (Scheme 1C). For these deuteration experiments, **2a,b** and 100 mol % of proline were mixed in DMSO- d_6 to which 1 vol % of D_2O had been added. Under otherwise identical experimental conditions, but in the absence of D_2O , we had observed the readily occurring retro-aldolization of **2a,b** as well as the presence of the rapidly interconverting²⁰ intermediates **4b,c,d** (Figure 2). Since both the retro-aldol reaction and the enamine–oxazolidinone exchange are associated with protonation in the α -position of the carbonyl compound, the α -deuteration of propionaldehyde **1a** and the derivatives thereof could be expected to proceed with ease in the presence of D_2O . Accordingly, an accumulation of deuterons in α' -position of **2a,b** and **3** should be observed over time (Figure 3A) and the comparison of the deuteration of the different species observed should provide insights into the actual formation pathway of **3**. To be able to connect this increasing degree of α' -deuteration, i.e., the ratio of 2H in α' -position, to the formation pathway of **3**, the direct α' -deuteration of the reaction products **2a,b** and **3** must be ruled out first. For **2a,b**, the lack of CH-acidity generally prevents α' -deuteration. In the case of **3**, direct vinylogous α' -deuteration was excluded by treating nondeuterated **3** with proline in DMSO/1 vol % of D_2O for more than 1 day: No α' -deuteration was observed (data not shown), which proves at the same time the irreversibility of the condensation under our experimental conditions. Thus, the degree

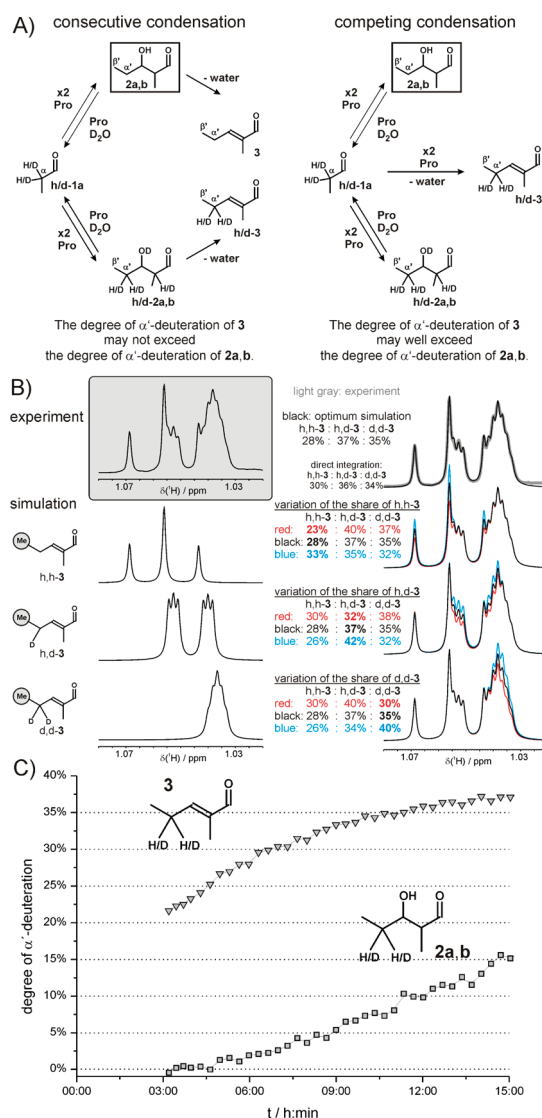


Figure 3. (A) Possible relationships of the aldol condensation with the aldol addition, with different implications for the relative degrees of α' -deuteration of **2a,b** and **3**. (B) Exemplary deconvolution of overlapping NMR resonances of differently deuterated species of the condensation product **3**. Displayed are the experimental spectral section (left top) as well as the underlying simulated spectra of the non-, mono-, and dideuterated compounds (left rows 2–4). For an estimation of the error range, the experimental spectrum and simulated spectra with varying ratios of the differently deuterated species are presented (right). (C) Experimentally determined degrees of α' -deuteration in the course of the formal dehydration of **2a,b** to **3** under catalysis of 100 mol % of proline in DMSO- d_6 with 1 vol % of D_2O at 300 K, supporting the general reaction scheme on the right-hand side of A). (Note: Data points for the first 3 h are not depicted because the amounts of **3** are so small, cf. Figure 2C, that an evaluation of the degree of deuteration is not reasonable.)

of α' -deuteration of **3** must be really caused by the degree of deuteration of the reaction intermediates involved.

To distinguish between the two fundamental reaction schemes (Figure 3A), the degrees of deuteration of the reaction products **2a,b** and **3** were evaluated. For **2a,b**, the loss of signal intensities of the α' -protons over time, compared to the aldehyde proton resonance, was ascribed to the deuteration and was hence used as

a measure for the degree of α' -deuteration. In the case of **3**, the β' -methyl proton resonance of the aldol acceptor moiety was used as a probe for the deuteration in the neighboring α' -position. On the basis of isotope-induced chemical shift changes of the β' resonance, the amounts of *h,h*-**3**, *h,d*-**3**, and *d,d*-**3** and, hence, the degree of α' -deuteration can be calculated after direct integration of the different branches of the β' resonance (see Figure 3B for an exemplary deconvolution of the experimental spectrum). The resulting degree of deuteration agrees very well with an exemplary simulation of the peak structure (Figure 3B, right top). The accuracy of this direct integration approach was furthermore supported by peak simulation with deviating shares of *h,h*-**3**, *h,d*-**3**, and *d,d*-**3**, respectively (see Figure 3B, right rows 2–4): Variations of the individual shares on the order of 5 percentage points would be easily detected despite the multiple resonance overlap. Accordingly, the error range of the degrees of deuteration of **3**, determined by this approach, can be estimated to be below 5 percentage points. On the basis of this good correspondence of the integration and the simulation, the more convenient integration method was used for the determination of the degrees of deuteration of **3**. The results of the evaluation of the degrees of deuteration of **2a,b** and **3** are shown in Figure 3C.

The comparison of the degrees of α' -deuteration of **2a,b** and **3** reveals substantially higher values for **3** than for **2a,b** throughout the reaction time observed. According to our above-mentioned argument, pathway I (Scheme 2A) can definitely be ruled out as the formation pathway of **3**. From this observation we can conclude that the proline-catalyzed condensation of aliphatic aldehydes does not proceed via the aldol addition and a consecutive dehydration step but rather represents a reaction pathway that competes with the aldol addition.

For the differentiation between pathways II and III, the rate-determining step of the aldol condensation should be clarified first. For the proline-catalyzed aldol addition, the C–C bond formation has been shown to be rate determining.^{19,41–43} Our experimental findings suggest the same for the aldol condensation: On the one hand, EXSY analyses²⁰ revealed that the formation of the enamine from the aldehyde via the oxazolidinones is a fast process (opposite to a study on the amino acid-catalyzed acetaldehyde self-condensation in aqueous and salt solution³⁰). In contrast, neither the aldol addition nor the aldol condensation product formation could be traced beyond the enamine by EXSY. On the other hand, the inability to detect species of type **6**, **7**, and **8** may be taken as an additional hint that the final elimination and hydrolysis steps are relatively rapid in comparison to the C–C bond formation. For the hydrolysis, this is covered experimentally by our EXSY findings²⁰ and also by the fact that the elimination is unlikely to be rate limiting.²⁷ Together with the above-mentioned correlation of the maximum formation rates of **3** with the maximum concentrations of **4b,c,d**, these experimental findings suggest that the C–C bond formation is rate determining in pathways II and III. Since both of these pathways of the aldol condensation share the same aldol acceptor species, a correlation of the concentration of **4a** to the formation rate of **3** is expected. To check this and hence to further support the assumption that the C–C bond formation is the rate-determining step in the proline-catalyzed aldol condensation, the progress of the aldol condensation was investigated for a sample of propionaldehyde **1a** and 100 mol % of proline in DMSO-*d*₆ with 0.5 vol % of D₂O at 300 K (Figure 4A). The concentration of the oxazolidinone **4b** was employed once more as a measure for the concentration of the aldol acceptor iminium

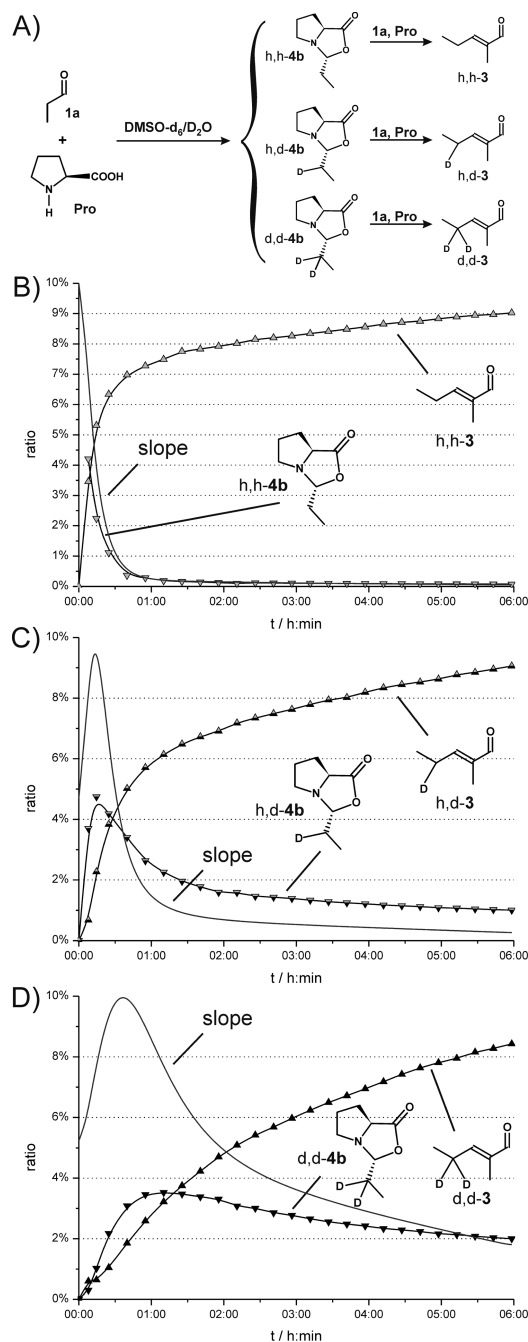


Figure 4. (A) Hypothetical formation of differently deuterated species of **3** via differently deuterated aldol acceptors (The oxazolidinone **4b** is shown as a representative for the typically postulated, yet undetected, iminium ion **4a**.) (B)–(D) Concentration curves of selected species in a reaction mixture of propionaldehyde with 100 mol % of L-proline in DMSO-*d*₆ with 0.5 vol % of D₂O at 300 K: (B) nondeuterated **4b** and **3**, (C) monodeuterated **4b** and **3**, and (D) dideuterated **4b** and **3** and, in each single case, the slope (displayed in arbitrary units) of the buildup curve of **3**, which corresponds to its formation rate. (Note: The total amount of C₃ moieties stemming from propionaldehyde, detected in the first spectrum, was set to 100%.)

ion **4a** (see above and Scheme 2B), and the slope of the concentration–time curve of **3** was again used as a measure for the formation rate of **3**. The beneficial effect of the addition of D₂O was an increase of the information density of our

investigation, in that three different aldol acceptors (*h,h*-4b, *h,d*-4b, *d,d*-4b) and three different condensation products (*h,h*-3, *h,d*-3, *d,d*-3) could be studied in parallel by using only one sample. The results of this experiment are depicted in Figure 4.

In the beginning of the reaction, *h,h*-4b is the only oxazolidinone present (Figure 4B). Then, the deuterated isotopologues *h,d*-4b and *d,d*-4b appear quite rapidly, reaching their maximum concentrations after about 20 min and 1 h, respectively (Figure 4C,D). Likewise, *h,h*-3 is the only condensation product formed in the beginning (Figure 4B), whereas the formation of *h,d*-3 and *d,d*-3 is retarded by an induction period (Figure 4C,D). In view of the convoluted proton spectra of the differently deuterated species and the associated deconvolution for the quantitative evaluation (see Figure 3B and Figure S5 in the Supporting Information), it is highly striking how well the maxima of the concentration of 4b and of the slope of 3 coincide in the cases of all three isotopologues (Figure 4B–D). This suggests according to the above-mentioned reasoning that the hypothetical iminium ion 4a (represented in its concentration–time curve by 4b) is in fact involved in the rate-determining step of the formation of 3 in our experimental system. Thus, the C–C bond formation should be the crucial and rate-determining step in the proline-catalyzed aldol condensation of aldehydes in DMSO.

Variation of the Catalyst Amount. With the knowledge that the proline-catalyzed aldol addition and aldol condensation are competing reactions and based on the experimentally supported assumption that the C–C bond formation is rate determining both in the condensation and in the addition pathway,^{19,41,42} there is now a possibility to differentiate between pathway II and pathway III: This option is due to the fact that both the aldol addition reaction and pathway II of the aldol condensation comprise one catalyst molecule in the rate determining step, either as the enamine 4d or as the iminium ion 4a. But in contrast, following pathway III, two catalyst molecules (4a and 4d) are involved in the rate-determining step of the aldol condensation.^{27,36,37} Thus, changes in the amount of catalyst should not have a significant impact on the competition between the aldol addition and the aldol condensation if the aldol condensation proceeds via pathway II. In contrast, if pathway III is operative for the aldol condensation reaction, lower catalyst amounts should initially favor the aldol addition, whereas higher catalyst amounts should increase the extent of the aldol condensation relative to the aldol addition. Revealing such different trends for the addition/condensation rate dependencies on the catalyst amount would thereby qualitatively confirm the detailed kinetic studies that have already proven the aldol condensation to be second order in the catalyst concentration.^{27,30}

To check this influence of the catalyst amount on the relative reaction rates of the aldol addition and condensation, different amounts of proline (10, 20, 50, and 100 mol %) were offered to propionaldehyde 1a in DMSO-*d*₆ at 300 K, and the progress of the reactions was followed by one-dimensional proton spectra. The interpolated yield of 2a,b and 3 after 30 min was used as a measure for the initial formation rates of 2a,b and 3, respectively. (Note: Retro-aldolization is expected to be negligible at early stages of the reaction and plotted against the varying amounts of L-Pro as the catalyst which are represented by the detected enamine concentration as a measure for the active amount of catalyst available to the system.⁴⁷) For all three dimer species, an increase in the initial formation rate is found with increasing amounts of proline. Without a doubt, another tendency becomes obvious from Figure 5 concerning the relative rates of the aldol

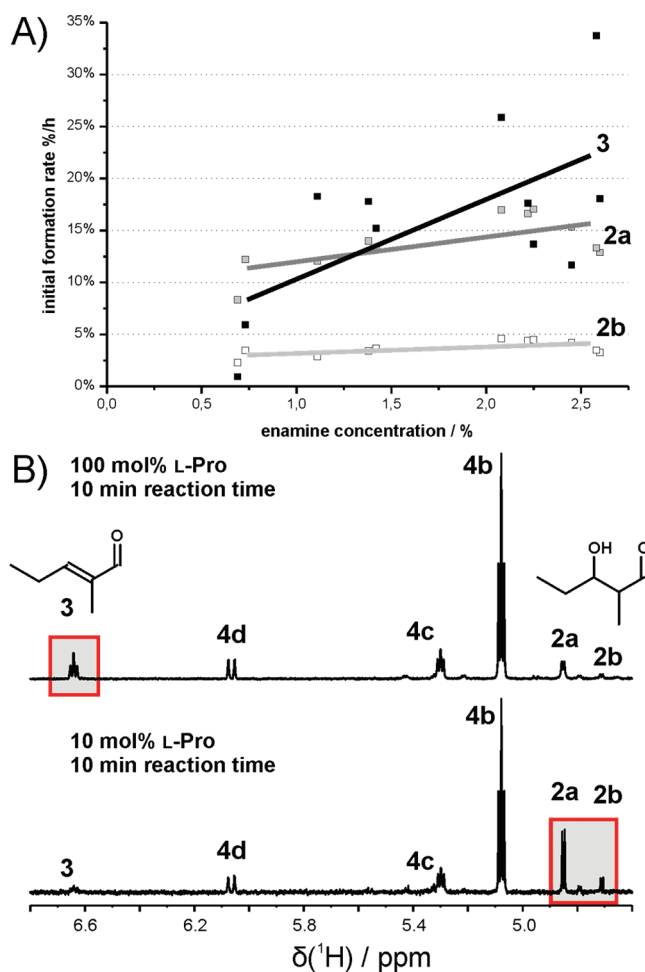


Figure 5. (A) Initial formation rates of the aldol products 2a,b and of the condensation product 3 in DMSO-*d*₆ at 300 K as a function of enamine concentration which represents the available, “active” amount of catalysts as offered to the system. (B) Direct comparison of representative ¹H NMR spectra of reaction mixtures subjected to 100 mol % (upper trace) and 10 mol % of L-Pro (lower trace) as catalyst taken at the same reaction time (10 min). The two regions of interest providing characteristic signals of the competing products 2 and 3 are highlighted within the spectra.

addition and condensation: While the condensation product 3 is formed more slowly than the addition products 2a,b at low catalyst concentration (10 mol %, enamine concentration ca. 0.7%), its formation is the fastest at high catalyst loadings (50 and 100 mol %, enamine concentration >2%). In addition, it is confirmed by the comparison of the initially formed quantities of 2a,b and 3 (cf. Figure S1C and S1D in the Supporting Information): While 2a,b exceeds 3 in the early stages of the aldol addition/condensation with low catalyst loadings (10 and 20 mol %), the formation of 3 is preferred over the one of 2a,b right from the beginning if higher amounts of catalyst (50 and 100 mol %) are used. This trend is exemplarily illustrated in Figure 5B. These qualitatively different acceleration tendencies of the aldol addition and aldol condensation indicate that different amounts of catalyst-derived species are involved in the rate determining steps of these reactions. Therefore, as elaborated above, pathway II can be ruled out as the pathway for the aldol condensation since, just like the aldol addition, it

requires one catalyst molecule in the C–C bond-forming step. In contrast, pathway III of the aldol condensation is associated with two catalyst-derived molecules in the rate-determining step. Thus, this pathway can well explain the stronger acceleration effect of the aldol condensation in comparison to the aldol addition upon increasing amounts of proline.

Hence we can provide further evidence that the proline-catalyzed aldol condensation of aldehydes proceeds via a double activation of both the aldol donor and the aldol acceptor molecule (pathway III in Scheme 2A). Since the enamine **4d** is readily detected in our study, there can be little doubt that it is involved as the aldol donor species in the formation of the condensation product **3**. On the other hand, the iminium ion **4a** has been typically proposed as the electrophilic aldol acceptor species. However, since the existence of this intermediate iminium zwitterion in solution has not been proven experimentally in proline-catalyzed reactions under our experimental conditions, one may well speculate about different electrophilically activated species acting as aldol acceptors, for instance, the carbinolamines (likewise undetected in our study) or the readily observed oxazolidinones. Further experimental and theoretical approaches will be necessary to shed more light on this unsolved issue of the proline-catalyzed aldol reaction. Likewise, more investigations will be necessary to clarify whether the aldol condensation might proceed via pathway IIIa or IIIb. We cannot further address this issue here since we have not been able to detect any of the intermediates of type **6**, **7**, or **8**.

Detection of an Acetaldehyde-Derived Proline–Dienamine.

Nevertheless, the observation that high proline loadings favor the Mannich-type aldehyde self-condensation over the aldehyde self-aldolization is supported by our findings on the proline-catalyzed self-aldolization/-condensation of acetaldehyde **9**. As reported previously,²⁰ the detection of the acetaldehyde-derived proline–enamine was not feasible because of the rapid progress of the proline-catalyzed self-aldolization reaction of acetaldehyde in DMSO. While this had largely impeded the use of acetaldehyde **9** as a nucleophilic reaction partner in amine-catalyzed crossed-aldol, Mannich or Michael reactions until recently,^{48–53} the proline-catalyzed asymmetric self-aldolization of **9** could be exploited synthetically to generate the triketide 5-hydroxy-2-hexenal **12**.³³ For this acetaldehyde trimerization, an aldol–Mannich cascade (Figure 6A, top)³³ as well as a Mannich–aldol sequence (Figure 6A, middle) are possible. In contrast, **13**, the condensation product of the trimerization of **9**, must be formed by two subsequent Mannich-type condensations (Figure 6A, bottom). Accordingly, while the formation of the triketide **12** was predominant at proline loadings on the order of 1 mol %, the condensation product **13** should be favored at higher proline amounts. To check this hypothesis, a reaction mixture of acetaldehyde **9** (*c* = 50 mM) and 100 mol % L-proline was prepared in DMSO-*d*₆ at 300 K and the progress of the reaction was monitored by 1D ¹H NMR spectra (Figure 6B).

Despite the complexity of the in situ NMR spectra of the reaction mixture, various rapidly vanishing species could be identified (because of the short lifetimes of all these species more detailed investigations could not be performed and their assignments are based on ¹H NMR data, see Figure S7 in the Supporting Information). Among them, two condensation products, the dimeric enal **10** and the trimeric **13** (Figure 6B), could be assigned reliably owing to their characteristic ¹H chemical shifts and multiplet patterns and in comparison with literature data.⁵⁴ Additionally, a butadienyl unit was recognized that can be assigned to **11**, the proline dienamine derived from **9**. In contrast,

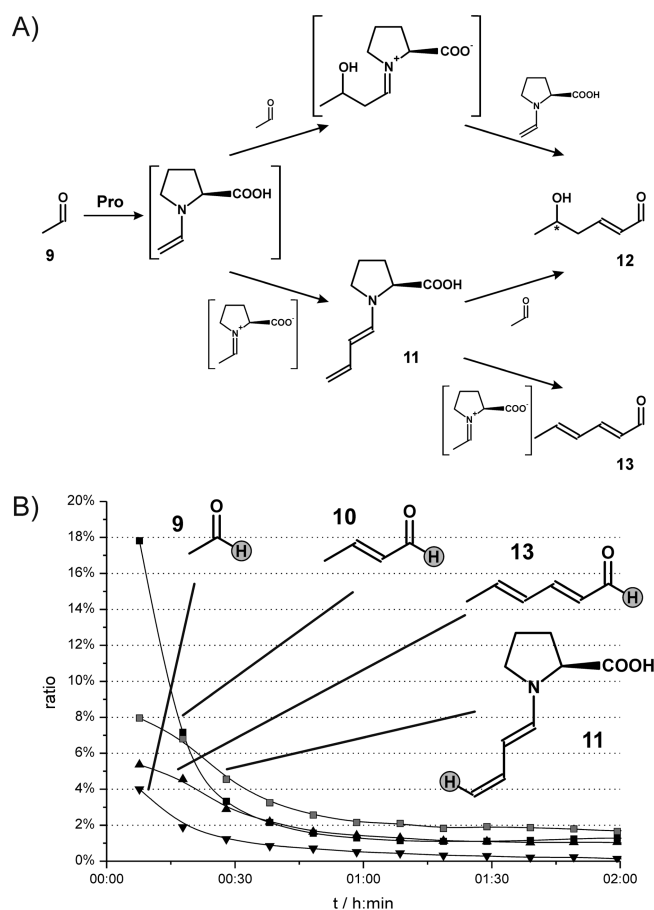


Figure 6. (A) Potential formation mechanisms of **12** via an aldol–Mannich³³ or via a Mannich–aldol cascade and of **13** via a Mannich–Mannich sequence. (B) Reliably assignable intermediates in the reaction mixture and the development of their concentrations over time. (Those protons whose resonances were used for the monitoring are highlighted in gray; see Figure S7 in the Supporting Information. Note: The total amount of C₂ units stemming from **9**, detected in the first spectrum, was set to 100%. However, because of the incomplete characterization of the whole of the reaction mixture, the actual ratios may be substantially lower.)

neither aldol dimers of **9** nor the triketide **12** were detected. Hence, the presence of the condensation dimer **10** and the absence of aldol dimers of **9** can be interpreted such that, for monomeric **9**, the Mannich-type condensation is favored over the aldol addition reaction when 100 mol % of proline is applied. The same conclusion can be drawn for the formation of trimers starting from **10**: The dienamine **11** should, as the common intermediate, in principle allow for the aldol addition to the triketide **12** and for the condensation to **13**. But only **13** is detected experimentally. Altogether, this preliminary study of the proline-catalyzed self-aldolization/-condensation in DMSO corroborates our finding that high proline loadings favor the aldol condensation over the competing aldol addition and that hence a Mannich-type mechanism with a 2-fold substrate activation underlies the condensation reaction. In addition, these investigations unearth the first in situ proline–dienamine. Thus, they should moreover guide the way toward the elucidation of mechanistic issues of the growing field of dienamine catalysis.^{55–62}

Time-Dependence of the Diastereoselectivity of the Aldol Addition. Another interesting finding of our studies, closely

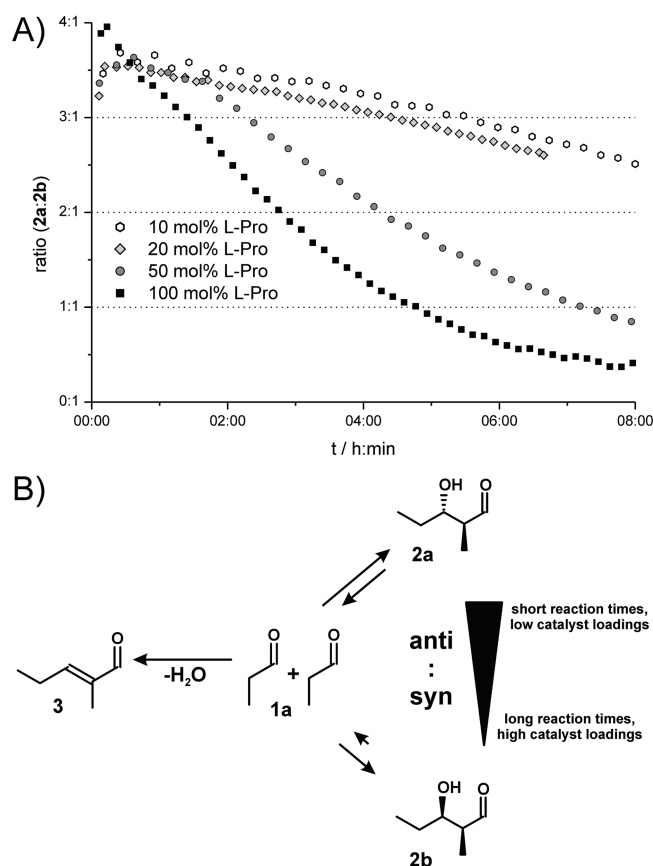


Figure 7. (A) Dependence of the product ratio 2a:2b of the proline-catalyzed self-aldolization of **1a** on the reaction time and on the amount of proline offered. (B) Graphical summary of the parameters and reaction pathways influencing the diastereoselectivity of the proline-catalyzed aldol addition of **1a**.

associated with the competitive nature of aldol addition and aldol condensation, concerns an issue that has not been addressed so far to our knowledge: the time-dependence of the diastereoselectivity of proline-catalyzed intermolecular aldol reaction of aldehydes. As can be seen from Figure 1B and 2A, the time-dependent appearance and vanishing is qualitatively different for the diastereomeric aldol products **2a** and **2b** in DMSO and in DMF alike (Figure S8 in the Supporting Information). In addition, Figure S1 (Supporting Information) reveals that these differences depend on the catalyst amount, too. As a synopsis of the experimental approaches discussed above, the ratio of the two aldol products **2a** and **2b**, hence the diastereoselectivity of the reaction, is depicted in Figure 7A as a function of reaction time.

For all catalyst amounts sampled, ranging from 10 to 100 mol %, a decrease of the ratio of **2a**:**2b** over time is observed. The more catalyst is employed, the steeper is this decay, for instance, with 100 mol % of proline, the diastereomeric ratio drops within 3 h from 4:1 to 2:1, with 50 mol % of proline, still a reduction from 3.5:1 to 1.75:1 within 5 h is observed. Unlike, at lower catalyst loadings (20 mol % and 10 mol %) the slope of the decreasing diastereoselectivity is very similar and only a slight offset of 0.2 to higher diastereomeric ratios is found for lower catalyst loading of 10 mol %. This time dependent loss of diastereoselectivity can be attributed to the different rates of the retro-aldolization of the aldol dimers **2a** and **2b** together with the competition of the aldol addition and the aldol condensation

for the monomeric species: The condensation withdraws the monomeric aldehyde (**1a**)-derived species of type **4** irreversibly from the equilibrium between aldolization and retro-aldolization. In addition, the retro-aldol reaction is significantly faster for the main aldolization product **2a** than for the minor product **2b** (see Figure 2A). Thus, upon retro-aldolization the competing irreversible condensation reaction causes the faster disappearance of the mainly formed **2a**, which in turn leads to a decrease in the diastereomeric ratio of the two aldol products. Since the rates of both the aldol addition (thus most probably also of the retro-aldol reaction) and the aldol condensation are enhanced by higher catalyst amounts but the rate of the aldol condensation significantly more (see Figure 5), the steeper decays in the selectivity–time curves with 50 and 100 mol % (Figure 7A) are readily rationalized.

Thus, highest diastereoselectivities can only be achieved if short reaction times are applied. However, in terms of a valuable and useful synthetic procedure the yield of the process is also crucial and might be affected in a detrimental way by such an experimental setup. Accordingly, only the combined optimum of both (diastereo)selectivity (Figure 7A) and yield (Figures 1B and S1, Supporting Information, for other catalyst loadings) can provide ideal reaction conditions. Use of the NMR reaction profiles points to other possible options for reaction optimization of the aldol addition investigated here. Again, for all catalyst loadings a decrease in diastereoselectivity for higher yields (conversion) is visible. In addition, depending on the amount of catalyst, different maximum yields can be reached and at a constant diastereoselectivity the yield increases using lower catalyst loadings.

Interestingly, the two plots presented in Figure 7A and 1B (product curves) correspond to direct information available from the reaction profiles mapping the products without any information about the reaction intermediates or the mechanism of the reaction. Accordingly, even in complex reactions with competing reaction pathways useful information for the optimization of the synthetic reaction conditions can be gained from simple NMR-reaction profiles of the products (for a further example using DMF-*d*₇ catalyst loading of mol %, see Figure S8, Supporting Information) that could serve as a valuable tool for the determination of optimal reaction parameters.

CONCLUSION

We have presented our NMR spectroscopic study on the proline-catalyzed self-condensation of aliphatic aldehydes in DMSO. By a detailed interpretation of the NMR-monitored reaction profiles of the condensation, starting from the monomeric aldehyde and from the aldol dimers, respectively, we have provided evidence that the aldol addition and the aldol condensation are *competing*, but not *consecutive* reaction pathways. This was deduced from the observation that the maximum formation rate of the condensation product does not correspond to the maximum concentration of the aldol addition products, but to the one of the aldehyde–proline adducts. This result was confirmed by the formal dehydration of the aldol dimers in the presence of proline and D₂O for which a higher degree of α' -deuteration of the condensation product was found in comparison to the aldol dimers. Additionally, it was observed that the acceleration of the aldol condensation by increasing the catalyst loading is more pronounced than for the competing aldol addition. Thus, it is concluded that two catalyst molecules are involved in the rate-determining step of the aldol condensation

which is suggested by our experimental findings to be the C–C bond formation. Accordingly, a Mannich-type reaction pathway, including the activation of both the aldol acceptor and the aldol donor, is indicated for the proline-catalyzed self-condensation of aldehydes. This can also rationalize the preference of the aldol condensation over the aldol addition when high amounts of catalyst are applied in the proline-catalyzed oligomerization of acetaldehyde. In this reaction mixture, the first in situ detection of a proline dienamine was accomplished. In addition, we could demonstrate the time-dependence of the stereoselectivity of the aldol addition, resulting from the competitive nature of the aldol addition and condensation. Extracting information from easily accessible NMR reaction profiles reveals that the yield (*anti*-aldol dimer **2a**) can be considerably improved by using low catalyst loadings with only a slight loss in diastereoselectivity during increased reaction times.

EXPERIMENTAL SECTION

All monitored reactions were conducted inside standard 5 mm NMR tubes by adding freshly distilled aldehyde **1a** or a mixture of **2a,b** or **3** (30 μ mol, each) to a suspension of L-proline (10, 20, 50, or 100 mol %) in 0.6 mL of DMSO- d_6 (optionally with 0.5 or 1 vol % of D₂O). The NMR tube was transferred to the spectrometer immediately after the mixing of all reacting components.

NMR measurements were performed at 300 K on two different NMR spectrometers (600.13 and 600.25 MHz), the latter equipped with a cryoprobe. NMR data were processed and evaluated with TOPSPIN 2.1, and the included DAISY software was used for the simulation of NMR spectra. The concentration–time curves of the observed aldol addition and condensation products were fit and its slope was calculated with the help of Origin 6.0.

The aldol dimers **2a,b** were synthesized according to a slightly modified literature procedure of MacMillan and co-workers.³⁹

ASSOCIATED CONTENT

S Supporting Information. Reaction profiles with varying amounts of catalyst as well as with butyraldehyde (including NMR spectra and assignments), observations on enal *E/Z*-selectivity, spectral deconvolution for partially deuterated **4b**, NMR spectrum and assignment of the reaction mixture with acetaldehyde, and time-dependent diastereoselectivity of the propionaldehyde aldol dimers in DMF. This material is available free of charge via the Internet at <http://pubs.acs.org>.

AUTHOR INFORMATION

Corresponding Author

*E-mail: kirsten.zeitler@chemie.uni-regensburg.de; ruth.gschwind@chemie.uni-regensburg.de

ACKNOWLEDGMENT

We are grateful to Johannes Franz for the synthesis of the aldol dimers **2a,b**. This work was supported by the DFG (SPP 1179). Scholarships by the Cusanuswerk and the Studienstiftung des deutschen Volkes are gratefully acknowledged.

REFERENCES

(1) Berkessel, A.; Gröger, H. *Asymmetric Organocatalysis - From Biomimetic Concepts to Applications in Asymmetric Synthesis*; Wiley-VCH: Weinheim, 2005.

- (2) Dalko, P. I., Ed. *Enantioselective Organocatalysis: Reactions and Experimental Procedures*; Wiley-VCH: Weinheim, 2007.
- (3) *Chem. Rev.* **2007**, *107*, 12: special issue on organocatalysis.
- (4) Reetz, M. T.; List, B.; Jaroch, S.; Weinmann, H.; Eds.; *Ernst Schering Foundation Symposium Proceedings "Organocatalysis"*; Springer: Berlin, 2008.
- (5) List, B., Ed. *Top. Curr. Chem.* **2010**, *291*: Asymmetric Organocatalysis.
- (6) List, B.; Lerner, R. A.; Barbas, C. F., III. *J. Am. Chem. Soc.* **2000**, *122*, 2395–2396.
- (7) List, B. *Chem. Commun.* **2006**, 819–824.
- (8) Mukherjee, S.; Yang, J. W.; Hoffmann, S.; List, B. *Chem. Rev.* **2007**, *107*, 5471–5569.
- (9) Melchiorre, P.; Marigo, M.; Carlone, A.; Bartoli, G. *Angew. Chem., Int. Ed.* **2008**, *47*, 6138–6171.
- (10) Bertelsen, S.; Jørgensen, K. A. *Chem. Soc. Rev.* **2009**, *38*, 2178–2189.
- (11) Pihko, P. M.; Majander, I.; Erkkilä, A. *Top. Curr. Chem.* **2010**, *291*, 29–75.
- (12) Nielsen, M.; Worgull, D.; Zweifel, T.; Gschwend, B.; Bertelsen, S.; Jørgensen, K. A. *Chem. Commun.* **2011**, *47*, 632–649.
- (13) Bahmanyar, S.; Houk, K. N. *J. Am. Chem. Soc.* **2001**, *123*, 11273–11283.
- (14) Bahmanyar, S.; Houk, K. N.; Martin, H. J.; List, B. *J. Am. Chem. Soc.* **2003**, *125*, 2475–2479.
- (15) Hoang, L.; Bahmanyar, S.; Houk, K. N.; List, B. *J. Am. Chem. Soc.* **2003**, *125*, 16–17.
- (16) Sharma, A.; Sunoj, R. *Angew. Chem., Int. Ed.* **2010**, *49*, 6373–6377.
- (17) List, B.; Hoang, L.; Martin, H. J. *Proc. Natl. Acad. Sci. U.S.A.* **2004**, *101*, 5839–5842.
- (18) Seebach, D.; Beck, A. K.; Badine, D. M.; Limbach, M.; Eschenmoser, A.; Treasurywala, A. M.; Hobi, R.; Priksosovich, W.; Linder, B. *Helv. Chim. Acta* **2007**, *90*, 425–471.
- (19) Zotova, N.; Broadbelt, L. J.; Armstrong, A.; Blackmond, D. G. *Bioorg. Med. Chem. Lett.* **2009**, *19*, 3934–3937.
- (20) Schmid, M. B.; Zeitler, K.; Gschwind, R. M. *Angew. Chem., Int. Ed.* **2010**, *49*, 4997–5003.
- (21) Bock, D. A.; Lehmann, C. W.; List, B. *Proc. Natl. Acad. Sci. U.S.A.* **2010**, *107*, 20636–20641.
- (22) Kanzian, T.; Lakhdar, S.; Mayr, H. *Angew. Chem., Int. Ed.* **2010**, *49*, 9526–9529.
- (23) Blackmond, D. G.; Moran, A.; Hughes, M.; Armstrong, A. *J. Am. Chem. Soc.* **2010**, *132*, 7598–7599.
- (24) For a recent GC-based investigation of aldol/Mannich ratios in the condensation of isobutyraldehyde with acetone, see: Domínguez de María, P.; Bracco, P.; Castelhano, L. F.; Bargeman, G. *ACS Catal.* **2011**, *1*, 70–75.
- (25) Trost, B. M.; Brindle, C. S. *Chem. Soc. Rev.* **2010**, *39*, 1600–1632.
- (26) Recently, the organocatalytic asymmetric Knoevenagel condensation has been introduced: Lee, A.; Michrowska, A.; Sulzer-Mosse, S.; List, B. *Angew. Chem., Int. Ed.* **2011**, *50*, 1707–1710.
- (27) Erkkilä, A.; Pihko, P. M. *Eur. J. Org. Chem.* **2007**, 4205–4216.
- (28) Zumbansen, K.; Döhring, A.; List, B. *Adv. Synth. Catal.* **2010**, *352*, 1135–1138.
- (29) List, B.; Pojarliev, P.; Castello, C. *Org. Lett.* **2001**, *3*, 573–575.
- (30) Nozière, B.; Córdova, A. *J. Phys. Chem. A* **2008**, *112*, 2827–2837.
- (31) Arend, M.; Westermann, B.; Risch, N. *Angew. Chem., Int. Ed.* **1998**, *37*, 1044–1070.
- (32) Ishikawa, T.; Uedo, E.; Okada, S.; Saito, S. *Synlett* **1999**, 450–452.
- (33) Córdova, A.; Notz, W.; Barbas, C. F., III. *J. Org. Chem.* **2002**, *67*, 301–303.
- (34) Casas, J.; Sundén, H.; Córdova, A. *Tetrahedron Lett.* **2004**, *45*, 6117–6119.
- (35) Smith, M. B.; March, J. *March's Advanced Organic Chemistry: Reactions, Mechanisms, and Structure*, 6th ed.; John Wiley & Sons, Inc.: Hoboken, 2006.

- (36) Hong, B.-C.; Wu, M.-F.; Tseng, H.-C.; Liao, J.-H. *Org. Lett.* **2006**, 8, 2217–2220.
- (37) Erkkilä, A.; Pihko, P. M. *J. Org. Chem.* **2006**, 71, 2538–2541.
- (38) A similar dual activation of carbonyl species by proline has recently been proposed for the organocatalytic homodimerization of enones: Guidi, V.; Sandoval, S.; McGregor, M. A.; Rosen, W. *Tetrahedron Lett.* **2010**, 51, 5086–5090.
- (39) Northrup, A. B.; MacMillan, D. W. C. *J. Am. Chem. Soc.* **2002**, 124, 6798–6799.
- (40) Miyano, M. *J. Org. Chem.* **1981**, 46, 1854–1857.
- (41) Zotova, N.; Franzke, A.; Armstrong, A.; Blackmond, D. G. *J. Am. Chem. Soc.* **2007**, 129, 15100–15101.
- (42) Zotova, N.; Moran, A.; Armstrong, A.; Blackmond, D. *Adv. Synth. Catal.* **2009**, 351, 2765–2769.
- (43) Interestingly, the rate-limiting step of the proline-catalyzed intramolecular Hajos–Parrish–Eder–Sauer–Wiechert^{44,45} aldol reaction has been shown to precede the C–C bond formation.⁴⁶ However, this may be attributed to the acceleration of the C–C bond formation by the “apparent concentration effect in the intramolecular case”.¹⁹
- (44) Eder, U.; Sauer, G.; Wiechert, R. *Angew. Chem., Int. Ed.* **1971**, 10, 496–497.
- (45) Hajos, Z. G.; Parrish, D. R. *J. Org. Chem.* **1974**, 39, 1615–1621.
- (46) Zhu, H.; Clemente, F. R.; Houk, K. N.; Meyer, M. P. *J. Am. Chem. Soc.* **2009**, 131, 1632–1633.
- (47) This type of graphical representation is used to show the clear trend of a strongly increasing formation rate for the condensation product **3** upon higher catalyst loadings in contrast to the nearly unchanging formation rates of the aldol products **2a,b** which are by far less affected by increasing catalyst amounts and only exceed the formation rate of the condensation product at the lowest catalyst loading (approximately 0.7% enamine concentration \approx 10 mol% of proline). Because of the limited solubility of proline in DMSO at amounts exceeding 30 mol % of catalyst loading and the influence of water on the reaction rates (enamine formation) as noticed by us and others,¹⁹ we found the relation of the formation rates against the actual present catalyst amount represented by the enamine concentration to be more accurate, especially in case of short reaction times. (Note: enamine formation is fast and reversible according to our earlier EXSY analyses.²⁰)
- (48) Alcaide, B.; Almendros, P. *Angew. Chem., Int. Ed.* **2008**, 47, 4632–4634.
- (49) García-García, P.; Ladépêche, A.; Halder, R.; List, B. *Angew. Chem., Int. Ed.* **2008**, 47, 4719–4721.
- (50) Hayashi, Y.; Itoh, T.; Aratake, S.; Ishikawa, H. *Angew. Chem., Int. Ed.* **2008**, 47, 2082–2084.
- (51) Hayashi, Y.; Itoh, T.; Ohkubo, M.; Ishikawa, H. *Angew. Chem., Int. Ed.* **2008**, 47, 4722–4724.
- (52) Hayashi, Y.; Okano, T.; Itoh, T.; Urushima, T.; Ishikawa, H.; Uchamaru, T. *Angew. Chem., Int. Ed.* **2008**, 47, 9053–9058.
- (53) Hayashi, Y.; Samanta, S.; Itoh, T.; Ishikawa, H. *Org. Lett.* **2008**, 10, 5581–5583.
- (54) <http://riodb01.ibase.aist.go.jp/sdbs/>, accessed March 11, 2011.
- (55) Bertelsen, S.; Marigo, M.; Brandes, S.; Diner, P.; Jørgensen, K. A. *J. Am. Chem. Soc.* **2006**, 128, 12973–12980.
- (56) Hong, B.-C.; Wu, M.-F.; Tseng, H.-C.; Huang, G.-F.; Su, C.-F.; Liao, J.-H. *J. Org. Chem.* **2007**, 72, 8459–8471.
- (57) Utsumi, N.; Zhang, H.; Tanaka, F.; Barbas, C. F., III. *Angew. Chem., Int. Ed.* **2007**, 46, 1878–1880.
- (58) de Figueiredo, R. M.; Fröhlich, R.; Christmann, M. *Angew. Chem., Int. Ed.* **2008**, 47, 1450–1453.
- (59) Liu, K.; Chougnet, A.; Woggon, W.-D. *Angew. Chem., Int. Ed.* **2008**, 47, 5827–5829.
- (60) Han, B.; Xiao, Y.-C.; He, Z.-Q.; Chen, Y.-C. *Org. Lett.* **2009**, 11, 4660–4663.
- (61) Marqués-López, E.; Herrera, R. P.; Marks, T.; Jacobs, W. C.; Könnig, D.; de Figueiredo, R. M.; Christmann, M. *Org. Lett.* **2009**, 11, 4116–4119.
- (62) Bencivenni, G.; Galzerano, P.; Mazzanti, A.; Bartoli, G.; Melchiorre, P. *Proc. Natl. Acad. Sci. U.S.A.* **2010**, 107, 20642–20647.